Multimetal Oxide Catalysts

DOI: 10.1002/ange.200902574

The ReaxFF Monte Carlo Reactive Dynamics Method for Predicting Atomistic Structures of Disordered Ceramics: Application to the Mo_3VO_x Catalyst**

*Kimberly Chenoweth, Adri C. T. van Duin, and William A. Goddard, III**

Multimetal oxides (MMO) often have partial or mixed occupation of some crystallographic sites making it difficult to examine atomistic processes, such as reactions and catalysis.[1] For example, X-ray powder diffraction data revealed that the MoVTeNbO catalyst which exhibits high activity for ammoxidation of propane to acrylonitrile consists of two phases (M1 and M2) where the highly active M1 phase (Supporting Information, Figure 1S) has 44 metal atoms per unit cell distributed among 12 crystallographically distinct sites plus 116 oxygen atoms per unit cell distributed over 30 sites.[1] The unit formula was refined to be $Mo^{V}_{0.55}Mo^{VI}_{6.76}V^{IV}_{1.52}V^{V}_{0.17}Te^{IV}_{0.69}Nb^{V}_{1.00}O_x$ $(28.34 < x < 28.69)$, however most Mo, V, and Te occupancies are fractional.[1e] Indeed four sites accounting for 11 metals per cell have V/Mo occupation ratios ranging from 0.26 to 0.62. Since V and Mo probably have very different reactivity and local oxygen environments, such partial occupations obscure the reaction mechanism of these systems, frustrating the development of improved catalysts. This problem of partial occupation is a common problem in important inorganic materials with no obvious experimental solution.

We propose herein a theoretical/computational approach to solving this problem. Our method involves starting with a supercell of the crystallographic unit cell, large enough to resolve all partial occupations into whole atoms. Next, we distribute the atoms over each type of crystallographic site so that the average occupation matches experiment. Then, we interchange any two atoms occupying the same crystallographic site and re-optimize the energy (with reactive dynamics (RD) and energy minimization (EM)). If the energy is improved, we keep the new structure and repeat the process for another pair of atoms. If the energy does not improve, we use a Monte Carlo (MC) criterion to determine whether the new structure is kept. This process is continued until the energy converges. This takes 500000 to 5000000 MC steps depending on the system. Next, we use a combination of RD and EM to optimize the structure while keeping the overall unit cell fixed. Since the supercells involved may contain 1000 to 10000 atoms and since it may be necessary to consider 500000 to 10000000 MC + RD steps, this computational approach is not yet practical for quantum mechanics (QM) calculations. However, it is practical for the ReaxFF reactive force field. We have developed ReaxFF to describe accurately reaction barriers and energetics of reactive processes for various metal–oxygen–carbon–hydrogen systems for which we have also shown that ReaxFF leads to accurate descriptions of various oxidation states of transition metals including V^0 to V^V, Mo^0 to Mo^{VI}, and Te^0 to Te^{VI},[2] all with the same force field. In addition, ReaxFF–RD have been carried out for systems involving 100000 to a million atoms showing that it is practical for this MC–RD procedure.[3]

Herein, we illustrate the ReaxFF–MC–RD structure refinement procedure for the Mo_3VO_x catalyst (Figure 1),[1a]

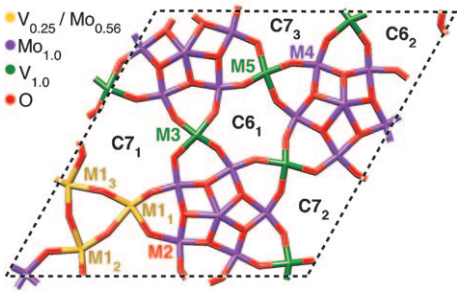

Figure 1. Crystal structure of the trigonal Mo_3VO_x catalyst.[1a] M = metal site, C = channel; see text for details.

which has a geometrical arrangement consistent with the M1 phase of the MoVTeNbO catalyst and has shown promise as an active and selective catalyst for the oxidization of propane to acrolein and acrylic acid as well as the oxidation of various alcohols.[1a,4] Mo_3VO_x, which is structurally less complex than the MoVTeNbOx catalyst, has 102 atoms per unit cell

[*] Prof. Dr. W. A. Goddard, III
Materials and Process Simulation Center, Division of Chemistry and Chemical Engineering, California Institute of Technology
Pasadena, CA 91125 (USA)
Fax: (+1) 626-585-0918
E-mail: wag@wag.caltech.edu
Homepage: http://www.wag.caltech.edu/
Prof. K. Chenoweth
Department of Chemistry, Smith College
Northampton, MA 01063 (USA)
Prof. A. C. T. van Duin
Department of Mechanical and Nuclear Engineering
Pennsylvania State University
University Park, PA 16802 (USA)

[**] We thank Prof. Ueda for a copy of ref. [1a], in advance of publication. Partial support was provided by DOE-EFRC (DE-PS02-08ER15944). The computational facilities were provided by grants from ARO-DARPA and ONR-DARPA.

Supporting information for this article (full computational details including the ReaxFF force field parameters) is available on the WWW under http://dx.doi.org/10.1002/anie.200902574.

distributed over nine crystallographically distinct metal sites of which just one possesses fractional occupancy (M1, Figure 1, involves three equivalent sites per cell). The reported occupancy at the M1 position is 56% Mo, 25% V, and 19% vacancy. In addition, there is a unique interlayer oxygen (Mo-O-Mo) with a fractional occupancy of 70% (one per cell). The Mo in the M2 site is one of the MO_6 units surrounding the Mo in the pentagonal channels. In addition, there are two hexagonal channels and three heptagonal channels that are empty. The Mo_3VO_x catalysts have similar structures and reactivities to the $MoVNbTeO_x$ catalysts, making it an ideal model system to gain insight into the structural features responsible for the observed reactivity in these catalysts.

To resolve the partial occupation at the M1 site, we doubled the unit cell to obtain a $1\times1\times2$ supercell (two layers with 204 atoms, $Mo_{40}V_{14}O_{150}$) with a total of six M1 sites. In the supercell, two of the six sites designated as V/Mo in Figure 1 are occupied by vanadium atoms to achieve the experimental fractional occupancy. This leads to three distinct configurations for the vanadium atoms including: 1) both vanadium atoms located at the same position, $M1_2$, in the first and second layer, 2) both vanadium atoms can be in the same layer, for example at positions $M1_2$ and $M1_1$, or 3) the first layer vanadium atom is at position $M1_2$ while the second layer vanadium atom is at position $M1_1$ (Figure 1).

We randomly choose one of the two vanadium atoms and interchange it with one of the four molybdenum atoms, optimize the structure, allowing the oxygen atom environments to relax. We found that the energy converged in 500000 steps (Supporting Information, Figure 2S). This process was carried out three times while varying the vanadium atoms among the M1 sites of the doubled unit cell. In each case, ReaxFF–MC–RD converged to the final structure obtained and shown in Figure 2, which exhibits configuration (1) with the vanadium atom in the first layer bound through an oxygen atom to a vanadium atom in the second layer. This arrangement leads to an ordered vertical V=O···V=O architecture similar to the V_2O_5[5a,b] and VOPO[5c–e] structures. In addition, we carried out simulations using larger supercells ($1\times2\times2$, $1\times2\times4$, and $2\times2\times2$) to evaluate the effect of increases in the number of potential configurations. In every case, the final structures had the vanadium atoms in site M1 ordered vertically through a bridging oxygen atom, indicating a strong preference for V–O–V over V–O–Mo.

The final structure ($1\times1\times2$ supercell) obtained from the MC simulation was fully minimized (to 1.5 kcal mol^{-1} Å^{-1} root mean square force) and 25 ps of ReaxFF–RD annealing was performed (fixed cell parameters using a Berendsen thermostat[6] or NVT, i.e. the number of particles N, the volume V, and the temperature T of the system are kept constant) to allow for optimization of the metal and oxygen sites. Next, we introduced a single oxygen vacancy into the structure, minimizing using ReaxFF, at each of the possible locations to determine the most stable site for the vacancy (which preferred the M2 site). Finally, 25 ps of ReaxFF–RD annealing was used to obtain a final structure for the Mo_3VO_x catalyst. This process resulted in the formula $Mo^{VI}_{34}Mo^{V}_{5}Mo^{IV}_{1}V^{V}_{9}V^{IV}_{5}O_{149}$ for the $1\times1\times2$ supercell (Figure 2a and Supporting Information, Figure 3S). The powder diffraction intensities (calculated using Mercury[7]) for this structure are consistent with the experimental intensities (Supporting Information, Figure 4S). To gain insight into the catalytic properties of this structure and to assign oxidation states to each of the metal sites, we analyzed bond orders, bond lengths, and metal coordination values.

Fully oxidized V^V atoms (M3, Figure 2a) have three single bonds to oxygen ($R_{V-O}\approx1.76$ Å) and one vanadyl oxygen atom ($R_{V=O}\approx1.51$ Å). In addition, the vanadyl groups are arranged in a chain ($O{=}V^{V}_{layer1}\cdots O{=}V^{V}_{layer2}$) along the *c* axis ($R_{V\cdots O}\approx3.2$ Å) as shown in the Supporting Information (Figure 5S). This stacking of vanadyl moieties is also observed in the V_2O_5 and VOPO structure.[5] Although V_2O_5-based catalysts exhibit a potential for alkane oxidative dehydrogenation (ODH), they tend to suffer from low selectivity and over-oxidation of the products.[8]

The vanadium atoms at site M3 bridge between heptagonal channel $C7_1$ and hexagonal channel $C6_1$, both of which contain reduced metal sites (one V^{IV} in $C7_1$ and one V^{IV} and four Mo^V in $C6_1$) surrounded by Mo^{VI} sites in the (001) plane, making this a plausible C–H activation site (Figure 1 and Figure 2a).

Other potential sites for C–H activation are the V^V sites ($M1_2$, Figure 2a) with a geometrical arrangement projecting vanadyl groups into the $C7_2$ heptagonal channel while bridging between heptagonal channels $C7_2$ and $C7_3$ (see Figure 5S).

Owing to the oxygen vacancy at M2 (Figure 2), we find a single reduced Mo^{IV} atom that is bound through an oxygen to a fully oxidized Mo^{VI} site in the second layer of the supercell. However ReaxFF–RD annealing (600 K) leads this Mo^{IV}-O-Mo^{VI} site to convert into Mo^{V}-O-Mo^{V}, indicating that the initial Mo^{IV} site in our structure is metastable. This finding is consistent with QM results for reduced Mo_3O_9 clusters (three MoO_2 units hooked together into a cycle through Mo–O–Mo bonds), in which the optimum structures lead to short Mo–Mo distances indicating a strong interaction between the reduced Mo^{IV} and Mo^{VI}.[9]

The $C6_1$ hexagonal channel contains Mo^{V}-O-Mo^{V} units in the *c* direction resulting in chains of partially reduced Mo atoms (M5, Figure 2). Owing to the reduced nature of these sites and the small size of the hexagonal channel, it is unlikely that the metal sites are responsible for the observed reactivity. However, they could play a secondary role in the selectivity of the catalyst through their inactivity providing active-site isolation and perhaps preventing over-oxidation or other side reactions that might be more likely in a channel with fully oxidized metal sites (i.e. $C7_1$, Figure 2). The Mo^{VI} sites in the catalyst consist of two Mo=O bonds ($R_{Mo=O}\approx1.77$ Å), two Mo–O bonds ($R_{Mo-O}\approx2.02$ Å), and two donor–acceptor Mo···O bonds ($R_{Mo\cdots O}\approx2.19$ Å). Such sites have been shown to convert allyl radicals into acrolein in the bismuth molybdate catalyst [9] suggesting that these sites may be important in selectivity for acrolein and acrylonitrile formation. By mapping out the location of the longer Mo–O bonds where the lone pair on the oxygen makes a donor–acceptor coordination to neighboring Mo, we were able to determine that there is a network of such interactions as shown in Figure 3. Mo^{VI} sites

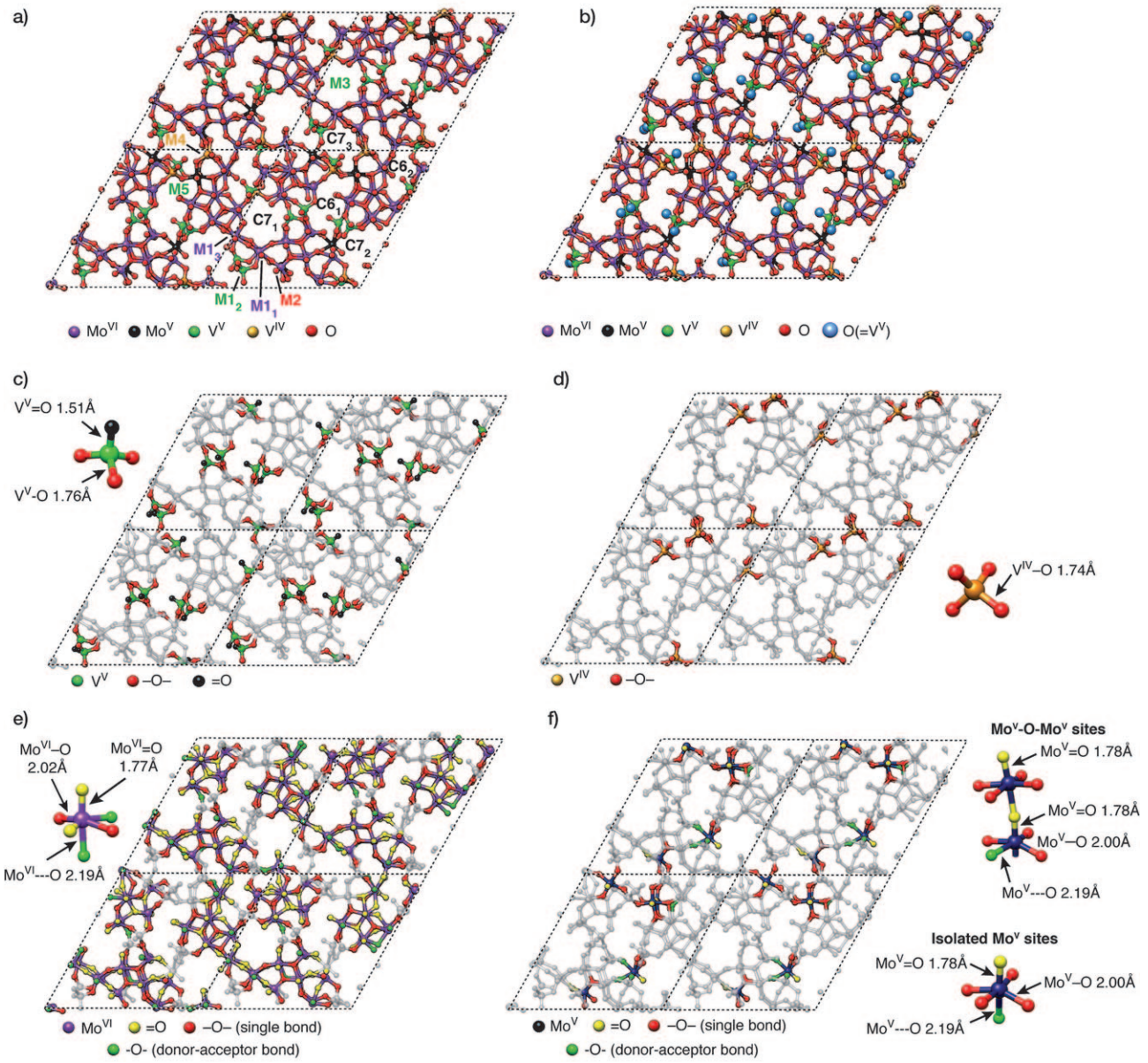

Figure 2. a) Final configuration of the trigonal Mo_3VO_x catalyst obtained from ReaxFF–MC–RD simulations. The oxidation states of metals are indicated by the various colors and the 1×1×2 supercell has been expanded in the *a* and *b* direction to 2×2×2. b) Arrangement of vanadyl oxygen atoms is shown in blue. In addition, the coordination environment, metal–oxygen bond length [Å], and location of c) V^V, d) V^{IV}, e) Mo^{VI}, and f) Mo^V is also shown.

maintain the network while other oxidation states or metals disrupt the donor–acceptor interactions especially in the *a*–*b* plane. The chains of Mo^{VI}=O···Mo^{VI} may participate in maintaining the oxidation state of the active sites located at the surface or in the channels.

To probe the reactivity of the ReaxFF Mo_3VO_x structure, we carried out a 50 ps ReaxFF–RD simulation on a six-layer slab with the (001) surface exposed to 20 propane molecules using a dual-temperature regime where the atoms of the MMO catalyst were kept at 300 K while the C and H atoms associated with the propane molecules were kept at 2000 K. (The procedure for surface preparation from the bulk structure is described in the Supporting Information with the initial and final configurations (Figure 6S) obtained from the ReaxFF–RD simulations.)

After 11.4 ps of simulation time, we found that two propane molecules (one from each side of the slab) started to diffuse into heptagonal channel $C7_2$ becoming completely contained in the channel after 12 ps. Then, a third propane molecule diffused into the same channel after an additional 5.25 ps. The average distance from the Mo and V metals to the centroid of the channel is 4.6 Å and the channel is approximately 18 Å in length. The cross-section of the Mo_3VO_X slab in Figure 4 shows that the neighboring heptagonal channel $C7_1$, which has fully oxidized metal sites except for one V^{IV}, remains empty. Although these channels are equilibrated

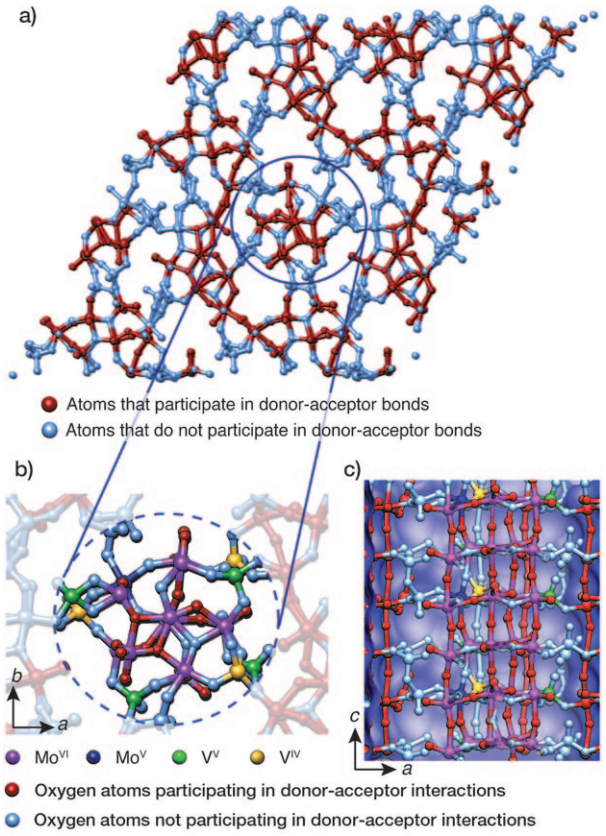

Figure 3. a) Network of donor–acceptor interactions (Mo^{VI}=O···Mo^{VI}) in the Mo_3VO_x catalyst where b) Mo^{VI} (purple) facilitates the continuation of the network while other metal sites disrupt the network. c) The network is more complete in the *c* direction compared to the *a*–*b* plane because of the chains of Mo^{VI}.

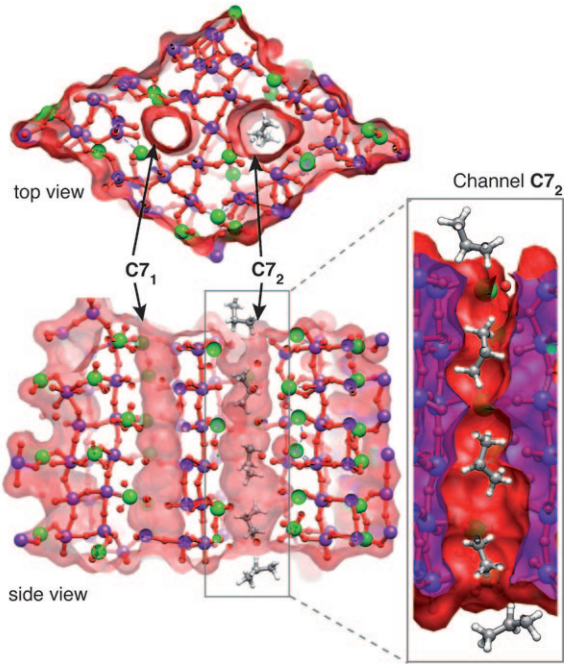

Figure 4. Cross-section of the final configuration from the propane/Mo_3VO_x ReaxFF–RD simulation illustrating the shape and size of heptagonal channels $C7_1$ and $C7_2$ from the top and side of the slab. Channel $C7_2$ with an average radius of 4.6 Å contains three propane molecules (channel length ca. 18 Å) while channel $C7_1$ is smaller with an average radius of 4.1 Å and remains empty.

crystallographically, they have become inequivalent as a result of the MC procedure which allows the V and Mo to coordinate to form the best structure. The result is that $C7_2$ has one V^{IV} and three Mo^V sites while $C7_1$ has only one V^{IV} while all others are fully oxidized. This structure can be compared to $C7_3$, which has the most reduced sites, containing three V^{IV} and four Mo^V. In addition, the size of $C7_2$ (based on the average distance of the Mo and V metals to the centroid of the channel) is 4.6 Å, compared to 4.1 Å for $C7_1$ and 3.8 Å for $C7_3$. Thus, the $C7_1$ and $C7_3$ channels may be too narrow to allow diffusion of hydrocarbons into the bulk. However, the high oxidation state of the metal sites near the pore openings might provide a site for propane activation.

Towards the end of the simulation ($t = 42.6$ ps) we observed one reactive event, where the methyl hydrogen of propane was abstracted by a V^V=O group on the (001) surface of the slab to form the *n*-propyl radical. This vanadyl group corresponds to position M5 in the bulk material, which bridges between heptagonal channel $C7_3$ and hexagonal channel $C6_1$ (Figure 1 and Figure 2). In the bulk, this vanadium metal site is in the reduced 4+ oxidation state, however creating the surface leads to a V^V=O unit on one interface while the other surface has a reduced vanadium site arising from breaking the V–O–V interlayer bond. This observation demonstrates that ReaxFF can be used to suggest potential reactive sites in these complex catalyst materials. In future studies, we aim to expand on these results by including the effects of experimental calcination treatments by exposing the surfaces to various sources of oxygen (O_2, O_3, H_2O, N_2O) and determine its effect on the catalytic properties of Mo_3VO_x.

We have presented a general computational methodology that can accurately resolve experimental partially occupied sites into equilibrated supercells optimized to take into account the distributions of neighboring metal atoms and oxygen atoms. This procedure provides the basis to examine the reaction mechanisms of these systems and allows for the investigation of key structure–reactivity relationships on the atomistic level that are responsible for catalyst performance.

Received: May 14, 2009
Published online: September 8, 2009

Keywords: heterogeneous catalysts · molecular dynamics · molybdenum · ReaxFF · vanadium

[1] a) M. Sadakane, N. Watanabe, T. Katou, Y. Nodasaka, W. Ueda, *Angew. Chem.* **2007**, *119*, 1515–1518; *Angew. Chem. Int. Ed.* **2007**, *46*, 1493–1496; b) T. Ushikubo, K. Oshima, A. Kayou, M. Hatano, *Stud. Surf. Sci. Catal.* **1997**, *112*, 473–480; c) P. DeSanto, Jr., D. J. Buttrey, R. K. Grasselli, C. G. Lugmair, A. F. Volpe, B. H. Toby, T. Vogt, *Top. Catal.* **2003**, *23*, 23–38; d) P. DeSan-

to, Jr., D. J. Buttrey, R. K. Grasselli, C. G. Lugmair, A. F. Volpe, Jr., B. H. Toby, T. Vogt, *Z. Kristallogr.* **2004**, *219*, 152 – 165; e) H. Murayama, D. Vitry, W. Ueda, G. Fuchs, M. Anne, J. L. Dubois, *Appl. Catal. A* **2007**, *318*, 137 – 142; f) D. Vitry, J. L. Dubois, W. Ueda, *J. Mol. Catal. A* **2004**, *220*, 67 – 76.

[2] a) W. A. Goddard III, A. van Duin, K. Chenoweth, M. J. Cheng, S. Pudar, J. Oxgaard, B. Merinov, Y. H. Jang, P. Persson, *Top. Catal.* **2006**, *38*, 93 – 103; b) W. A. Goddard III, K. Chenoweth, S. Pudar, A. C. T. van Duin, M. J. Cheng, *Top. Catal.* **2008**, *50*, 2 – 18; c) K. Chenoweth, A. C. T. van Duin, P. Persson, M. J. Cheng, J. Oxgaard, W. A. Goddard III, *J. Phys. Chem. C* **2008**, *112*, 14645 – 14654; d) K. Chenoweth, A. C. van Duin, W. A. Goddard III, *J. Phys. Chem. A* **2008**, *112*, 1040 – 1053.

[3] a) A. Nakano, R. K. Kalia, K. Nomura, A. Sharma, P. Vashishta, F. Shimojo, A. C. T. van Duin, W. A. Goddard III, R. Biswas, D. Srivastava, *Comput. Mater. Sci.* **2007**, *38*, 642 – 652; b) P. Vashishta, R. K. Kalia, A. Nakano, *J. Phys. Chem. B* **2006**, *110*, 3727 – 3733.

[4] a) N. Watanabe, W. Ueda, *Ind. Eng. Chem. Res.* **2006**, *45*, 607 – 614; b) W. Ueda, D. Vitry, T. Kato, N. Watanabe, Y. Endo, *Res. Chem. Intermed.* **2006**, *32*, 217 – 233; c) F. Wang, W. Ueda, *Chem. Lett.* **2008**, *37*, 184 – 185.

[5] a) H. G. Bachmann, F. R. Ahmed, W. H. Barnes, *Z. Kristallogr. Krist.* **1961**, *115*, 110 – 131; b) M. J. Cheng, K. Chenoweth, J. Oxgaard, A. van Duin, W. A. Goddard III, *J. Phys. Chem. C* **2007**, *111*, 5115 – 5127; c) V. V. Guliants, *Catal. Today* **1999**, *51*, 255 – 268; d) G. J. Hutchings, *J. Mater. Chem.* **2004**, *14*, 3385 – 3395; e) D. Thompson, B. K. Hodnett, *Top. Catal.* **2008**, *50*, 116 – 123.

[6] H. J. C. Berendsen, J. P. M. Postma, W. F. van Gunsteren, A. DiNola, J. R. Haak, *J. Chem. Phys.* **1984**, *81*, 3684 – 3690.

[7] C. F. Macrae, P. R. Edgington, P. McCabe, E. Pidcock, G. P. Shields, R. Taylor, M. Towler, J. Streek, *J. Appl. Crystallogr.* **2006**, *39*, 453 – 457.

[8] S. Surnev, M. G. Ramsey, F. P. Netzer, *Prog. Surf. Sci.* **2003**, *73*, 117 – 165.

[9] a) J. N. Allison, W. A. Goddard III, *ACS Symp. Ser.* **1985**, *279*, 23 – 36; b) Y. H. Jang, W. A. Goddard III, *J. Phys. Chem. B* **2002**, *106*, 5997 – 6013; c) S. Pudar, J. Oxgaard, K. Chenoweth, A. C. T. van Duin, W. A. Goddard III, *J. Phys. Chem. C* **2007**, *111*, 16405 – 16415.

